Published in final edited form as:
Science. 2010 July 30; 329(5991): 538–541. doi:10.1126/science.1189345.

Tissue-Engineered Lungs for in Vivo Implantation

Thomas H. Petersen[1,2], **Elizabeth A. Calle**[1], **Liping Zhao**[3], **Eun Jung Lee**[3], **Liqiong Gui**[3], **MichaSam B. Raredon**[1], **Kseniya Gavrilov**[4], **Tai Yi**[5], **Zhen W. Zhuang**[6], **Christopher Breuer**[5], **Erica Herzog**[6], and **Laura E. Niklason**[1,3,*]

[1]Department of Biomedical Engineering, Yale University, New Haven, CT 06520, USA.

[2]Department of Biomedical Engineering, Duke University, Durham, NC 27708, USA.

[3]Department of Anesthesia, Yale University, New Haven, CT 06520, USA.

[4]Department of Cellular and Molecular Physiology, Yale University, New Haven, CT 06520, USA.

[5]Department of Surgery, Yale University, New Haven, CT 06520, USA.

[6]Department of Internal Medicine, Yale University, New Haven, CT 06520, USA.

Abstract

Because adult lung tissue has limited regeneration capacity, lung transplantation is the primary therapy for severely damaged lungs. To explore whether lung tissue can be regenerated in vitro, we treated lungs from adult rats using a procedure that removes cellular components but leaves behind a scaffold of extracellular matrix that retains the hierarchical branching structures of airways and vasculature. We then used a bioreactor to culture pulmonary epithelium and vascular endothelium on the acellular lung matrix. The seeded epithelium displayed remarkable hierarchical organization within the matrix, and the seeded endothelial cells efficiently repopulated the vascular compartment. In vitro, the mechanical characteristics of the engineered lungs were similar to those of native lung tissue, and when implanted into rats in vivo for short time intervals (45 to 120 minutes) the engineered lungs participated in gas exchange. Although representing only an initial step toward the ultimate goal of generating fully functional lungs in vitro, these results suggest that repopulation of lung matrix is a viable strategy for lung regeneration.

Lung diseases account for some 400,000 deaths annually in the United States (1). Human lungs do not generally repair or regenerate beyond the microscopic, cellular level. Currently, the only way to replace lung tissue is to perform lung transplantation, which is an expensive procedure that achieves only 10 to 20% survival at 10 years and one that is hampered by a severe shortage of donor organs (2). Recently, techniques have been developed to quantitatively decellularize complex organs such as heart, liver, and kidney (3–5). Acellular matrices can provide attractive scaffolds for repopulation with lung-specific cells for lung engineering because the extracellular matrix template should contain appropriate three-dimensional (3D) architecture and regional-specific cues for cellular adhesion. To be functional in vivo, an engineered lung should (i) contain lung-specific cells, (ii) display the branching geometry of the airways and contain a perfusing microvasculature, (iii) provide

*To whom correspondence should be addressed. laura.niklason@yale.edu.

Supporting Online Material www.sciencemag.org/cgi/content/full/science.1189345/DC1 Materials and Methods SOM Text Figs. S1 to S11 Table S1 References

barrier function to separate blood from air, and (iv) have mechanical properties that allow ventilation at physiological pressures.

Here, we describe our progress toward the construction of a functional tissue-engineered lung, using rat as a model system. Our approach is summarized in Fig. 1. We first decellularized native lung tissue in order to remove all immunogenic cellular constituents (Fig. 1, A and B). We found that after careful decellularization, the tissue retained its alveolar micro-architecture, its ability to function as a barrier to particulates, and its tissue mechanics. Repopulation of the acellular lung matrix with mixed populations of neonatal lung epithelial cells resulted in regional-specific epithelial seeding in correct anatomic locations. To enhance the survival and differentiation of lung epithelium, we cultured the matrix in a bioreactor designed to mimic certain features of the fetal lung environment, including vascular perfusion and liquid ventilation (Fig. 1, C and D) (6). Lastly, we tested the functionality of the engineered lung tissue by implanting it for short time periods in a syngeneic rat model (Fig. 1E).

Preparation of a decellularized lung scaffold

We harvested lung tissue from adult Fischer 344 rats and treated the lungs in the vascular and airway compartments with detergent solutions (Fig. 1 and movie S1). The decellularization solution contains 3-[(3-cholamidopropyl)dimethylammonio]-1-propanesulfonate (CHAPS), a zwitterionic detergent, in a phosphate buffer at 1.0 M salt concentration (7). Vascular perfusion pressure was maintained below 20 mmHg, with total time of tissue exposure typically in the range of 2 to 3 hours. Analysis of the decellularized lung matrices by means of high-resolution micro-computed tomography (micro-CT) revealed intact lung architecture and an intact arterial tree and microvasculature (Fig. 2, A to C). The cells and nuclear material were removed with the decellularization process, but the alveolar septal architecture remained undisturbed (Fig. 2, E and F). Fluorometric DNA assay confirmed that approximately 99% of DNA was removed by the decellularization process (Fig. 2G), and immunoblotting for major histocompatibility complex I and II (MHC-I and MHC-II) as well as β-actin confirmed that decellularized lung matrices were depleted of these cellular markers (Fig. 2D). Scanning electron microscopy (SEM) confirmed that alveolar cells, red blood cells, and cellular proteins present in native lung were absent in the decellularized scaffold (Fig. 2, H and I, and fig. S3). Analysis of the matrix by means of transmission electron microscopy (TEM) revealed that the ultrastructure of the alveolar septae and the delicate microvessels surrounding the alveoli remained intact (Fig. 2J and fig. S3). Immunofluorescence and histochemical staining indicated that collagen, elastin, and laminin were preserved in decellularized matrices (figs. S4 and S5). Additionally, quantitative assays showed that extracellular matrix collagen was preserved, whereas elastin was partially depleted by the decellularization process (40% of elastin remains in acellular matrices), and sulfated glycosaminoglycans (GAGs) were >90% removed (Fig. 2G and fig. S4). Hence, the lung decellularization protocol produces an acellular matrix scaffold that retains the gross, microstructural, and ultrastructural properties of native lung, yet removal of antigenic cellular components is essentially complete.

Properties of the lung bioreactor

The lung bioreactor contains a main reservoir in which the decellularized lung is mounted, using cannulae that are inserted into the trachea and pulmonary artery (fig. S1A). Culture medium is perfused into the pulmonary artery at physiological pressures (fig. S1B) (7). To provide negative-pressure ventilation of the engineered lung, a syringe pump withdraws a defined volume of air from the main bioreactor to create a negative pressure (Fig. 1C and figs. S1C and S2). Lung inflation under negative pressure is accompanied by inhalation of

liquid medium from a trachea reservoir via a “breathing loop.” For exhalation, the syringe pump returns air to the main reservoir, causing lung exhalation of liquid medium into the trachea reservoir.

To repopulate the decellularized matrix, we injected cells into the vascular or airway compartments, or both, and maintained the matrix in culture for up to 8 days (Fig. 1C). This produced an engineered lung tissue that could then be removed from the bioreactor for further analysis or that could be orthotopically transplanted into a rat recipient (Fig. 1, D and E).

Repopulation of acellular matrix to produce an engineered lung

Seeding of the decellularized matrix with mixed populations of neonatal rat lung epithelial cells (fig. S7) into the airway compartment generally resulted in good adherence of the cells to alveolar structures, as well as to small- and medium-sized airways (Fig. 3A). Microvascular lung endothelial cells, when injected into the pulmonary artery of acellular scaffolds, adhered throughout the scaffold vasculature (Fig. 3B). Seeded pulmonary epithelial cells replicated rapidly and rarely displayed markers of apoptotic cell death (Fig. 3, C and D), despite the difficulty in culturing such cells on standard tissue culture plastic in vitro (8). This observation suggests that substrate cues on the acellular lung matrix are important for pulmonary epithelial cell attachment and replication.

In the biomimetic bioreactor, vascular perfusion greatly enhanced endothelial adhesion and survival on the lung matrix (fig. S9, A and B). Negative pressure ventilation had multiple beneficial effects on cultured lung epithelium, including enhanced survival of epithelium in distal alveoli and clearance of epithelial secretions from the airway tree (fig. S9, C to F). Clearance of airway secretions through ventilation indicates that the developing epithelium is in communication with the airway tree and is not growing randomly within the matrix. In addition, ventilation with air—as opposed to with culture medium—increased the numbers of type I alveolar epithelial cells, as well as the numbers of ciliated columnar epithelial cells (fig. S9, G to J). Engineered lungs also produce pro-surfactant proteins B and C (pro-SPB, pro-SPC), although we could not detect mature SPB (Fig. 3E). Surfactant proteins are critical for reducing alveolar surface tension and enabling lung inflation at physiologically normal pressures.

We performed compliance testing on the engineered lungs under quasi-static conditions by injecting air into the lungs and monitoring resultant pressure changes. Typical compliance curves for native lung, acellular matrix, and repopulated engineered lungs are shown in Fig. 3, F to H. The compliance values were, respectively, 0.35 ± 0.08 (n = 10 measures), 0.09 ± 0.02 (n = 4 measures), and 0.14 ± 0.06 (n = 5 measures) mL/mmHg (mean ± SD, P < 0.001 for difference between native and both decellularized and engineered compliances). Compliance values were measured at initial filling of the lungs (arrowheads in Fig. 3, F to H), and thus lower compliances for decellularized matrix and engineered lung mean that these two tissues have higher “opening pressures,” and less functional surfactant, than does native lung. Despite this difference, the overall stress-strain relationships and the ultimate tensile stresses were similar between the three groups (Fig. 3I and fig. S6). Thus, no substantial stiffening or weakening of the extracellular matrix occurs in the repopulated, engineered lungs as compared with native adult lungs.

To evaluate the distribution and phenotype of cells in the engineered lungs, we performed fluorescent immunohistochemical staining (fig. S8). Endothelial cells seeded into the vasculature were extensively distributed and expressed CD-31, as did comparable cells in native rat lung (fig. S8A). TEM analysis revealed the presence of tight junctions within the engineered endothelium, which is consistent with the development of some barrier function

(fig. S10). With respect to the seeded lung epithelium, Clara cell secretory protein (CCSP)–positive cells, which in native lung are found in small airways, were found primarily in very small airway structures after 4 days and in larger structures after 8 days in engineered lungs (fig. S8B). Pro-SPC, a marker of type II alveolar epithelium, is normally present at the vertices of alveoli in native lung. In the engineered lungs, pro-SPC expression was diffuse in alveoli and in small airways after 4 days of culture, but at 8 days it showed a more native expression pattern at the vertices of alveoli (fig. S8C). In contrast, aquaporin-5—a specific marker for type I epithelium—was found diffusely throughout native alveoli and in engineered lungs after 4 days but was largely absent after 8 days (fig. S8D). This observation is consistent with previous work on neonatal rat development, which showed that type I cells do not fully differentiate until the post-natal period, when air breathing commences (9). Indeed, engineered lungs that were ventilated with air, as opposed to liquid culture medium, displayed more aquaporin-5 expression in alveoli after 8 days of culture (fig. S9, G and H) and also contained sparse ciliated epithelial cells (fig. S9, I and J). Additional cell types noted included mesenchymal cells and the airway epithelial progenitor basal cells (fig. S8, E and F). Hence, the engineered lungs contained many of the important cell types of native lung tissues. In addition, the spatial distribution of the various cell types was regional-specific, and with extended culture periods in the bioreactor the overall pattern of cellular distribution and differentiation became more similar to that in native lung tissue.

To determine whether the decellularization and repopulation methodologies used in our studies of rat lungs were applicable to human tissues, we obtained human lung segments from a tissue bank and treated them with decellularization solutions for up to 6 hours (7). Histological staining showed that complete cellular removal was achieved, with preservation of alveolar architecture (fig. S11, A and B). We seeded the acellular matrices with A549 human epithelial carcinoma cells and endothelial cells derived from human cord-blood endothelial progenitor cells (7). The A549 cells adhered well to alveolar surfaces, and the endothelial cells adhered to the vasculature (fig. S11, C and D), supporting the notion that these approaches may also be applicable to human lung tissues.

Implantation of engineered lungs into rats

To determine whether engineered rodent lungs were implantable and functional for gas exchange, we performed orthotopic left lung transplantation in four animals (7). Acellular matrices were seeded with neonatal rat lung epithelium and lung microvascular endothelium and cultured for approximately 1 week in the bioreactor. For lung implantation, the native lungs were exposed via left thoracotomy, and the left lung was excised. After anticoagulation with heparin, the left mainstem bronchus, left pulmonary vein, and left pulmonary artery of the engineered lung were anastomosed to the recipient, the lung was ventilated with 100% oxygen, and blood flow was reestablished.

In all cases, the engineered lungs were easily suturable to the recipient and were ventilated with no visible air leak from the parenchyma (Fig. 4A and movie S2). All engineered lungs became perfused with blood over a period of seconds to minutes, with blood visibly turning from dark to bright red as the hemoglobin became oxygenated. Implantation times for engineered lungs ranged from 45 min to 2 hours. After perfusion and ventilation, blood gas samples were drawn from the pulmonary artery, left and right pulmonary veins (veins were clamped and samples drawn from each lung individually), and the unclamped pulmonary vein so as to document the extent of gas exchange occurring in the native and engineered lungs (Table 1).

Chest x-ray confirmed that the engineered lung was inflated with air, but the level of inflation was less than that of the native right lung (Fig. 4B). Histological evaluation of

explanted engineered lungs revealed red blood cells in large blood vessels and septal microvessels, and some bleeding into airways, although this was modest (Fig. 4C). Blood gas analysis revealed that the tissue-engineered lungs were effective in exchanging oxygen and carbon dioxide (Table 1). Partial pressures of oxygen (PO_2) increased from 27 ± 7 mmHg in the pulmonary artery to 283 ± 48 mmHg in the left pulmonary vein, indicating complete hemoglobin saturation and oxygenation. Hemoglobin saturation was 100% for both engineered left lung and native right lung venous samples. In addition, carbon dioxide removal was efficient, with CO_2 falling from 41 ± 13 mmHg in the pulmonary artery to 11 ± 5 mmHg in the left, engineered pulmonary vein. Although the PO_2 in the right pulmonary vein was higher than in the left (634 ± 69 versus 283 ± 48 mmHg), this difference may not be of substantial physiological consequence because hemoglobin saturation is complete above oxygen pressures of 100 mmHg (10).

Discussion

To date, cell therapy and tissue engineering have been applied less extensively to lung than to other tissues and organs (11–13). Many efforts in lung regeneration have involved synthetic scaffolds or simple in vitro culture systems. Such systems can regenerate certain microscopic features of alveolar architecture but have not yet produced tissue that can participate in gas exchange (14, 15). Use of the decellularization paradigm for respiratory tissue was described in 2008, when Macchiarini and colleagues implanted a reseeded tracheal matrix into a patient with severe bronchomalacia (16).

In the current work, we have demonstrated the feasibility of producing an engineered lung that displays much of the microarchitecture of native lung and that can effect gas exchange for short periods of time when implanted into rats. Although these results are encouraging, multiple issues remain to be addressed before long-term engineered lung function can be realized. For example, alveolar barrier function must be improved so as to prevent any leakage of blood components into the airways. This can be accomplished through iterative improvement in the decellularization procedure in order to minimize alveolar septal damage (17). Production of surfactant should be increased (18), and differentiated columnar ciliated epithelium should be enhanced by more prolonged air breathing in culture (19). In addition, the efficiency of vascular endothelial coverage must be very high throughout the engineered lung vasculature. This is to prevent exposure of collagen-containing basement membrane to the circulation, with consequent thrombosis, because some clotting was noted at explant. Lastly, a decellularization strategy for lung regeneration will only become clinically useful when a suitable, autologous source of pulmonary epithelium can be identified, such as a resident lung stem cell or induced pluripotent stem cell (20–24).

Supplementary Material

Refer to Web version on PubMed Central for supplementary material.

Acknowledgments

We thank M. Colehour for help with bioreactor development and Western blotting, R. Homer for histologic assessment, and B. Stripp for the CCSP antibody. This work was funded by Yale University Department of Anesthesia and by NIH grant HL 098220 (to L.E.N.). T.H.P. is supported by NIH T32 GM007171. L.E.N. holds stock in Humacyte, a regenerative medicine company. The authors (L.E.N., T.H.P., and E.A.C.) and Yale University have filed a patent application related to tissue engineering of lungs.

References and Notes

1. American Lung Association. [accessed 4 March 2010] Lung Disease Data 2008. www.lungusa.org

2. Orens JB, Garrity ER Jr. Proc. Am. Thorac. Soc. 2009; 6:13. [PubMed: 19131526]
3. Ott HC, et al. Nat. Med. 2008; 14:213. [PubMed: 18193059]
4. Gilbert TW, Sellaro TL, Badylak SF. Biomaterials. 2006; 27:3675. [PubMed: 16519932]
5. Baptista PM, et al. IEEE Eng. Med. Biol. Soc. 2009; 31:6526.
6. Inanlou MR, Baguma-Nibasheka M, Kablar B. Histol. Histopathol. 2005; 20:1261. [PubMed: 16136506]
7. Materials and methods are available as supporting material on Science Online.
8. Sporty JL, Horálková L, Ehrhardt C. Expert Opin. Drug Metab. Toxicol. 2008; 4:333. [PubMed: 18433340]
9. Massaro D, Teich N, Maxwell S, Massaro GD, Whitney P. J. Clin. Invest. 1985; 76:1297. [PubMed: 4056033]
10. Staub, NC. Physiology. Berne, RM.; Levy, MN., editors. Vol. 4. Mosby; St. Louis: 1998. chaps. 32 and 33
11. Andrade CF, Wong AP, Waddell TK, Keshavjee S, Liu M. Am. J. Physiol. Lung Cell. Mol. Physiol. 2007; 292:L510. [PubMed: 17028264]
12. Cortiella J, et al. Tissue Eng. 2006; 12:1213. [PubMed: 16771635]
13. Mondrinos MJ, et al. Tissue Eng. 2006; 12:717. [PubMed: 16674286]
14. Sugihara H, Toda S, Miyabara S, Fujiyama C, Yonemitsu N. Am. J. Pathol. 1993; 142:783. [PubMed: 8456939]
15. Lin YM, Boccaccini AR, Polak JM, Bishop AE, Maquet V. J. Biomater. Appl. 2006; 21:109. [PubMed: 16443629]
16. Macchiarini P, et al. Lancet. 2008; 372:2023. [PubMed: 19022496]
17. DeFouw DO. Am. Rev. Respir. Dis. 1983; 127:S9. [PubMed: 6846951]
18. Bittar, EE. Pulmonary Biology in Health and Disease. Springer; New York: 2002.
19. Gray TE, Guzman K, Davis CW, Abdullah LH, Nettesheim P. Am. J. Respir. Cell Mol. Biol. 1996; 14:104. [PubMed: 8534481]
20. Wang D, Morales JE, Calame DG, Alcorn JL, Wetsel RA. Mol. Ther. 2010; 18:625. [PubMed: 20087316]
21. Yu J, et al. Science. 2007; 318:1917. [PubMed: 18029452]
22. Kim CF, et al. Cell. 2005; 121:823. [PubMed: 15960971]
23. Rippon HJ, et al. Proc. Am. Thorac. Soc. 2008; 5:717. [PubMed: 18684724]
24. Roszell B, et al. Tissue Eng. Part A. 2009; 15:3351. [PubMed: 19388834]

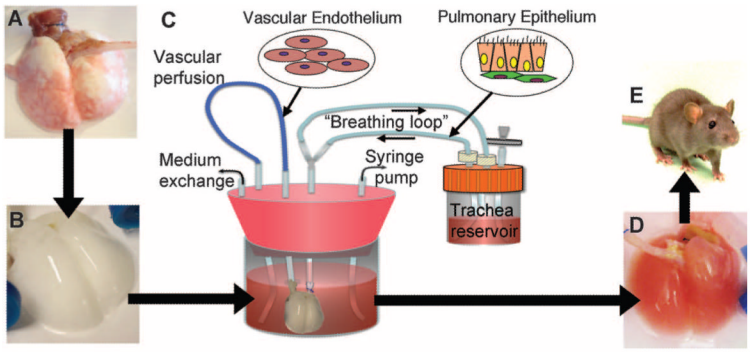

Fig. 1.

Schema for lung tissue engineering. (**A**) Native adult rat lung is cannulated in the pulmonary artery and trachea for infusion of decellularization solutions. (**B**) Acellular lung matrix is devoid of cells after 2 to 3 hours of treatment. (**C**) Acellular matrix is mounted inside a biomimetic bioreactor that allows seeding of vascular endothelium into the pulmonary artery and pulmonary epithelium into the trachea. (**D**) After 4 to 8 days of culture, the engineered lung is removed from the bioreactor and is suitable for implantation into (**E**) the syngeneic rat recipient.

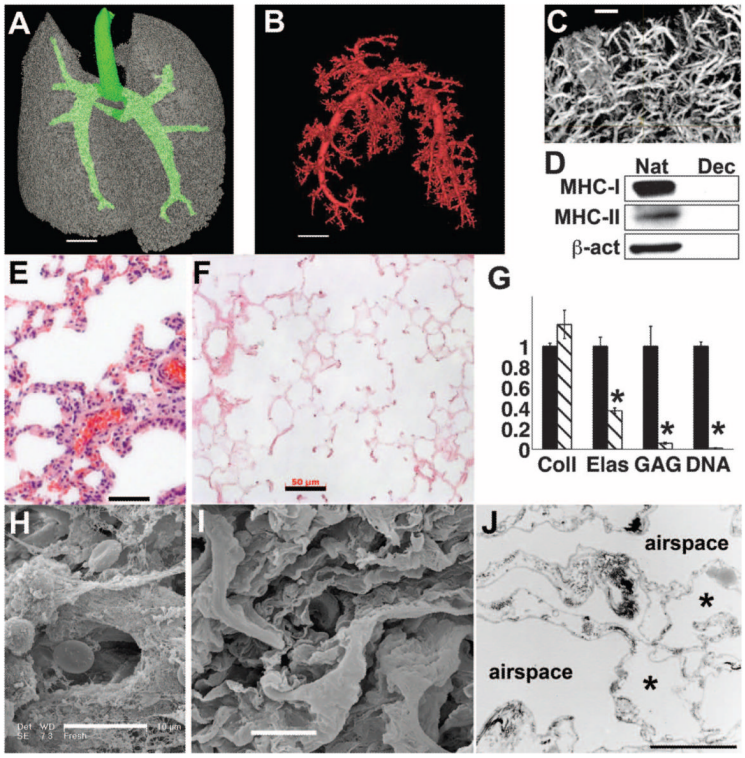

Fig. 2.

Characterization of acellular lung matrix. (**A**) 3D micro-CT of the acellular matrix airway compartment. Large airways are in green. (**B**) Micro-CT angiography of vascular compartment, thresholded to visualize only large vessels. In (A) and (B), voxel size is 58 μm; scale bar, 4 mm. (**C**) Micro-CT angiography of smaller vessels in acellular lung. Voxel size, 6.5 μm; scale bar, 500 μm. (**D**) Immunoblot for MHC-1, MHC-II, and β-actin in native (Nat) and decellularized (Dec) lungs, showing removal of cellular proteins. (**E**) Hematoxylin and eosin (H&E) stain of native rat lung. (**F**) H&E stain of acellular lung matrix. Scale bar, 50 μm in (E) and (F). (**G**) Collagen (Coll), elastin (Elas), glycosaminoglycan (GAG), and DNA contents of native lung (black bars) and acellular matrices (hatched bars). Values are mean ± SD per lung (n ≥ 4 lungs for all measures), scaled to 1 for native, with asterisk indicating $P < 0.05$ for difference between native and acellular matrices. (**H**) SEM of native rat lung. (**I**) SEM of acellular matrix. Scale bar, 10 μm in (H) and (I). (**J**) TEM of acellular lung matrix. Asterisk indicates capillaries in alveolar septa. Scale bar, 5 μm.

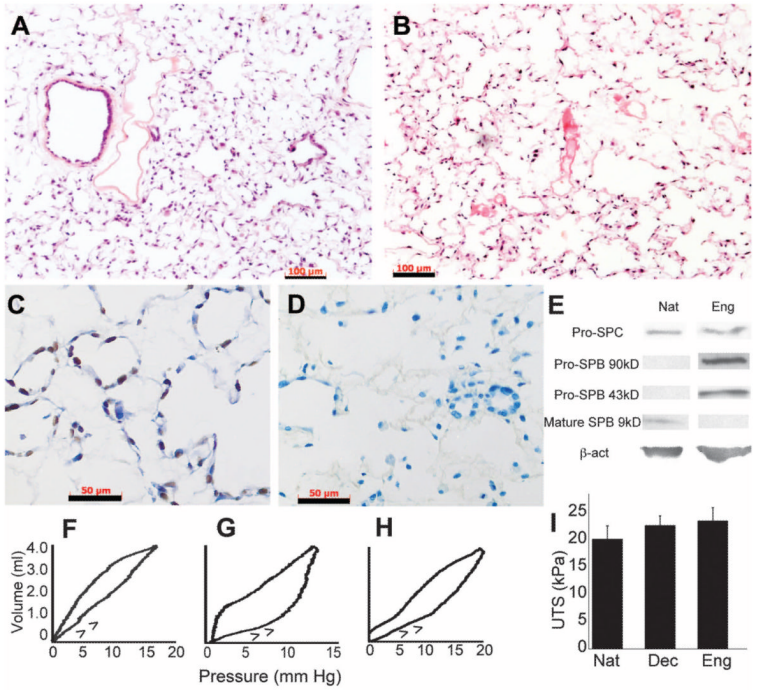

Fig. 3.

Repopulation of the matrix with lung epithelial and endothelial cells and mechanical assessment of the engineered lungs. (**A**) H&E stain of mixed neonatal pulmonary epithelium seeded into acellular matrix and cultured for 8 days. (**B**) H&E stain of lung microvascular endothelium seeded into vascular compartment and cultured for 8 days. Scale bars, 100 μm in (A) and (B). (**C**) Proliferating cell nuclear antigen stain of epithelial culture after 8 days; brown nuclei are dividing. (**D**) Terminal deoxynucleotidyl transferase–mediated deoxyuridine triphosphate nick end labeling stain of epithelium after 4 days of culture detects no apoptotic cells (positive cells stain brown; green indicates nuclear counterstain). Scale bars, 50 μm in (C) and (D). (**E**) Immunoblots for pro-SPC indicates similar expression for native (Nat) and engineered (Eng) lung. Engineered lung expresses SPB precursor proteins at 43 and 90 kD, but no mature SPB. β-actin confirms similar protein loading. (**F** to **H**) Quasi-static compliance curves for (F) typical native, (G) acellular, and (H) engineered lungs; arrows indicate inflation arm of loop. (**I**) Mean ultimate tensile strengths (UTS) of native ($n = 4$), acellular ($n = 10$), and engineered ($n = 5$) lungs. Error bars are SD; there were no significant differences between any groups.

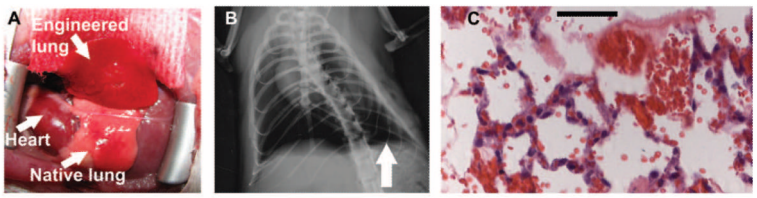

Fig. 4.

Implantation of engineered lungs into rats. (**A**) Tissue-engineered left lung was implanted into adult Fischer 344 rat recipient and photographed ~30 min later. (**B**) X-ray image of rat showing the implanted engineered left lung (white arrow) and the right native lung. (**C**) H&E stain of explanted lung. Red blood cells perfusing septa are evident, and some red blood cells are present in airspaces. Scale bar, 50 μm.

Table 1

Gas exchange in engineered lungs implanted into rats. Shown are blood gas values and oxygen saturations for samples taken from rats implanted with an engineered lung. Values are mean ± SD; $n = 3$ samples for each sample type except for right pulmonary vein, in which $n = 2$ samples. Sat, saturation.

Sample location	pH	PO_2 (mmHg)	O_2 Sat (%)	PCO_2 (mmHg)
Pulmonary artery	7.30 ± 0.06	27 ± 7	44 ± 20	41 ± 13
Right pulmonary vein	7.53 ± 0.08	634 ± 69	100 ±0	20 ± 1
Left (implant) pulmonary vein	7.68 ± 0.28	283 ± 48	100 ± 0	11 ± 5
Mixed pulmonary veins	7.58 ± 0.08	495 ± 174	100 ± 0	18 ± 3